Hindawi Publishing Corporation
EURASIP Journal on Advances in Signal Processing
Volume 2010, Article ID 126082, 12 pages
doi:10.1155/2010/126082

Research Article

Hybrid RSS-RTT Localization Scheme for Indoor Wireless Networks

A. Bahillo,[1] S. Mazuelas,[1] R. M. Lorenzo,[2] P. Fernández,[2] J. Prieto,[2] R. J. Durán,[2] and E. J. Abril[2]

[1] *CEDETEL (Center for the Development of Telecommunications), Edificio Solar, Parque Tecnológico de Boecillo, 47151 Boecillo (Valladolid), Spain*
[2] *Department of Signal Theory and Communications and Telematic Engineering, University of Valladolid, Paseo Belén 15, 47011 Valladolid, Spain*

Correspondence should be addressed to A. Bahillo, abahillo@cedetel.es

Received 16 September 2009; Revised 22 January 2010; Accepted 10 March 2010

Academic Editor: Fredrik Gustafsson

Nowadays, a variety of information related to the distance between two wireless devices can be easily obtained. This paper presents a hybrid localization scheme that combines received signal strength (RSS) and round-trip time (RTT) information with the aim of improving the previous localization schemes. The hybrid localization scheme is based on an RSS ranging technique that uses RTT ranging estimates as constraints among other heuristic constraints. Once distances have been well estimated, the position of the mobile station (MS) to be located is estimated using a new robust least-squared multilateration (RLSM) technique that combines the RSS and RTT ranging estimates mitigating the negative effect of outliers. The hybrid localization scheme coupled with simulations and measurements demonstrates that it outperforms the conventional RSS-based and RTT-based localization schemes, without using either a tracking technique or a previous calibration stage of the environment.

1. Introduction

Intense research work is recently being carried out to design and build localization schemes that can operate in indoor environments and achieve a degree of accuracy, reliability, and cost comparable to the well-known Global Navigation Satellite Systems (GNSS). Accurate indoor localization is an important challenge for commercial, public safety, and military applications [1, 2]. In commercial applications for residential and nursing homes, there is an increasing need to track people with special needs, such as children and elderly people who are out of regular visual supervision, navigate the blind, and find specific items in warehouses. For public safety and military applications, indoor localization systems are needed to track inmates in prisons or navigate police officers, fire fighters, and soldiers to complete their missions inside buildings. Among the many technological possibilities that have been considered for indoor localization schemes such as infrared, ultrasonic, and artificial vision,radiofrequency-based schemes predominate today due to their availability, low cost, and coverage range.

The purpose of localization schemes is to find the unknown position of a mobile station (MS) given a set of measurements. The localization process consists of two main steps. Firstly, selected localization metrics between the MS and the reference points or anchors are performed. Secondly, these metrics are processed through a positioning algorithm to estimate the location coordinates of the MS. As the measurements of metrics become less reliable, the complexity of the positioning algorithm increases. The localization metrics may be classified into two broad categories: direction-based and range-based systems. Direction-based systems utilize antenna arrays and angle of arrival (AOA) estimation techniques to infer the MS position [3], while the received signal strength (RSS) and the time of arrival (TOA) of the received signals are the metrics used for range-based techniques [4–7]. The possibility of combining different localization metrics encourages to

develop hybrid schemes that exploit the complementary behavior of metrics to improve the overall accuracy of the localization schemes. For instance, in [8] the Cramér-Rao Bound (CRB) on location estimation accuracy of two different hybrid schemes based on the combination of RSS and either TOA or TDOA (Time Difference Of Arrival) measurements is computed, concluding that, for short-range networks, the hybrid schemes offer improved accuracy with respect to conventional TOA and TDOA schemes. In [9] an algorithm of neural networks is implemented for the hybrid scheme that combines RSS and TOA measurements, enhancing the overall performance of the hybrid localization scheme. As range-based methods need measurements from more than two anchors for positioning in two dimensions, AOA measurements are incorporated to reduce the network overload. For instance, a hybrid algorithm is presented by incorporating AOA data in a time-based method, needing measurements from only two anchors for line-of-sight (LOS) [10] and non-LOS (NLOS) environments [11].

Time-based and direction-based measurements are highly correlated with the MS position [3, 12], but AOA and TOA localization metrics are not available to inexpensive and common wireless systems, due to the need for antenna arrays and time synchronization or complex timing requirements, respectively. On the contrary, the RSS indicator is widely available and provides a cost-effective means of position estimation, although in indoor environments the propagation phenomena cause the RSS localization metric to poorly correlate with distance [12]. The aim of this paper is to provide a new hybrid strength time-based method for indoor localization that takes advantage of easily available RSS measurements and does not need time synchronization thanks to RTT (Round-Trip Time) measurements. A previous essay [13] proposes a hybrid localization scheme that combines RSS and RTT measurements. However, it is implemented for open areas, taking RTT measured values from the cellular network and TOA measured values from GNSS. As indoor environments impose more technological challenges than open areas, in this paper, a new hybrid RSS-RTT localization scheme that operates in indoor environments and in common IEEE 802.11 wireless networks is proposed to overcome indoor impairments and improve the accuracy of the MS location estimation with respect to RTT-only and RSS-only schemes. In order to do that, the RSS and RTT measurements are carried out at the MS that is going to be located by using the printed circuit board (PCB) proposed in [14].

The paper is divided as follows: Section 2 provides an overview of the RTT-based and RSS-based ranging techniques. Section 3 describes the new hybrid RSS-RTT ranging technique, providing important simulation results. Section 4 describes a new multilateration technique that combines RSS and RTT range estimates to find the MS position. This section also includes simulation results and measurements inside a building. Finally, conclusions are summarized in Section 5.

2. Previous Work

Ranging techniques have significant effects on location accuracy and system complexity [12, 15]. This section outlines the previous work related to two ranging techniques whose performance was individually evaluated: RSS-based and RTT-based ranging methods.

2.1. RSS-Based Ranging. RSS ranging is based on the principle that says that the greater the distance between two wireless nodes is, the weaker their relative received signals are. However, the relationship between the RSS values and the distance depends on a large number of unpredictable factors. In fact, small changes in position or direction may result in dramatic differences in RSS values. The attenuation caused by the distance that separates two wireless nodes is known as path-loss, and it is modeled to be inversely proportional to the distance between the emitter and the receiver raised to a certain exponent. This exponent is known as path-loss exponent [16]. Other factors that affect RSS values are the multipath or fast fading factor and the shadowing or slow fading factor. These two factors can be modeled with Rayleigh or Rician and log-normal distributions [17, 18], respectively. However, the fast fading term can be eliminated by averaging the RSS values over a time interval [19].

Following the derivation steps shown in [20] the RSS values can be modeled by the following expression:

$$P_{R_i} = P_{\text{ref}} - 10n_i \log_{10}(d_i) + X, \tag{1}$$

where d_i is the actual distance between the MS and the anchor A_i, P_{ref} is the power measured at a reference distance and it depends on several factors: averaged fast and slow fading, antennas gains, and transmitted power. In practice, P_{ref} can be often known beforehand [21] and its value will be valid as long as the antenna gains and the transmitted power remain constant. The term n_i is the path-loss exponent corresponding to the path connecting the MS to the anchor A_i, while X denotes a zero mean Gaussian random variable caused by slow fading. The conventional textbook explanation for the slow fading is the multiplicative model which assumes that there are several random multiplicative factors attenuating the received signal, and the logarithm of their product approaches the Gaussian distribution for a sufficiently large number of such factors [22]. The expression (1) has been widely used in the literature to describe RSS values as a function of the distance between two wireless nodes. Common examples of the use of this expression are the known propagation models of Okumura-Hata or Egli [16].

Theoretical and/or empirical RSS-based range models could mold the dependence between the RSS values and the distance. In a previous work [5], the expression for the maximum likelihood estimator (MLE) of the distance was derived from the expression (1). Assuming that the MS could obtain RSS values in time instants $t_1, t_2, \ldots, t_N$, where (t_1, t_N) is a time interval in which we can assume that the distance and the environment between the MS and the anchor A_i

do not change significantly, the MLE of the distance can be determined from RSS values as follows.

$$\hat{d}_{\mathrm{RSS}_i} = 10^{(P_{\mathrm{ref}} - \overline{P_{R_i}})/10n_i}, \tag{2}$$

where $\hat{d}_{\mathrm{RSS}_i}$ is the estimated distance from the MS to the anchor A_i, P_{ref} is the power measured at the reference distance of one meter, $\overline{P_{R_i}}$ is the received power from the anchor A_i averaged over the time interval (t_1, t_N), and n_i is the path-loss exponent. The difference between the estimated and the actual distances is defined as the range estimate error, where the variance of this error is at least as high as the inverse of the Fisher information. For analytical details on computing the CRB and the Fisher information see [5]. The expression (2) is used to obtain range estimates from RSS values once the parameters P_{ref} and n_i are known. As mentioned above, P_{ref} is easy to obtain from a few RSS measurements taken in a place of reference and it can be assumed to be constant, as long as the antenna gains and the transmitted power also remain constant. However, assuming n_i as a constant would be a simplification of reality because propagation conditions between the MS and the anchor are unpredictable and could change abruptly in time. For this reason, the values of n_i that characterize the propagation environment between the MS and each anchor have to be dynamically updated. In [5] the values of n_i are updated at each time interval (t_1, t_N) based on maximizing an objective function. This objective function quantifies the compatibility of all the range estimates between the MS and each anchor as follows:

Let (A_{x_i}, A_{y_i}) be the known positions of the M anchors being $i = 1, 2, \ldots, M$ with $M \geq 3$. In the event that all range estimates are precise, the M circles with (A_{x_i}, A_{y_i}) centers and $\hat{d}_{\mathrm{RSS}_i}$ radius would intersect at a single point. That point is the result of solving an overdetermined system of M quadratic equations whose least squares solution is defined as $(\tilde{x}, \tilde{y})$. Therefore, the M circles would cut at a single point, if and only if,

$$(\tilde{x} - A_{x_i})^2 + (\tilde{y} - A_{y_i})^2 - \hat{d}^2_{\mathrm{RSS}_i} = 0, \quad i = 1, 2, \ldots, M. \tag{3}$$

However, in the general case, as all the range estimates are not precise, the M circles do not intersect at a single point. It is clear that the further the equations of the expression (3) differ from zero the further the M circles would cut at a single point. In this case, solving (3) requires significant complexity, and it is difficult to analyze. Therefore, instead of using the circles as the equations to determine $(\tilde{x}, \tilde{y})$, the radical axes of all pairs of circles can be used. The radical axis of two circles is the locus of points at which tangents drawn to both circles have the same length. Analytically, the radical axis can be easily obtained by subtracting the two circles equations involved. Thus, the complex problem of solving an over-determined system of M quadratic equations is reduced to solve an over-determined system of $M(M-1)/2$ linear equations defined by the radical axes.

The compatibility function of the group of M range estimates is defined as the extent to which the $M(M-1)/2$ radical axes cut at a single point. Analytically,

$$C\left(\hat{d}_{\mathrm{RSS}_1}, \hat{d}_{\mathrm{RSS}_2}, \ldots, \hat{d}_{\mathrm{RSS}_M}\right) = -\sum_{i=1}^{M}\left(\frac{(\tilde{x} - A_{x_i})^2 + (\tilde{y} - A_{y_i})^2}{\hat{d}^2_{\mathrm{RSS}_i}} - 1\right)^2, \tag{4}$$

where C is the compatibility function, the squares sum is weighted with each range estimate in order to apply more relevance to the smaller one, and the minus sign indicates that the sum of squares and the compatibility are inversely related. The expression (4) depends only on the path-loss exponents n_i used to estimate distances from RSS values according to the expression (2). Hence, the path-loss exponents that best characterize the different paths connecting the MS to the anchors A_i could be estimated as the values $\hat{n}_1, \hat{n}_2, \ldots, \hat{n}_M$ that maximize the compatibility expressed in (4). Analytically:

$$\begin{aligned}(\hat{n}_1, \hat{n}_2, \ldots, \hat{n}_M) &= \arg \max_{(n_1, n_2, \ldots, n_M)} C(n_1, n_2, \ldots, n_M) \\ &= \arg \min_{(n_1, n_2, \ldots, n_M)} \\ &\quad \times \sum_{i=1}^{M}\left(\frac{(\tilde{x} - A_{x_i})^2 + (\tilde{y} - A_{y_i})^2}{\hat{d}^2_{\mathrm{RSS}_i}} - 1\right)^2.\end{aligned} \tag{5}$$

The expression (5) is a nonlinear least squares problem that can be solved by using the Levenberg-Marquardt algorithm [23, 24], where a rough approximation of the path-loss exponents such as $n_i = 2$, for all i can be chosen as an initial guess. Indeed, the problem formulation is an iterative process that starts by choosing an initial guess for the path-loss exponents n_i, $i = 1, 2, \ldots, M$, and whose values will be modified iteratively with the aim of minimizing the expression (5). The process of updating the $\hat{n}_1, \hat{n}_2, \ldots, \hat{n}_M$ values finishes when the expression (5) is equal to zero or the maximum number of iterations has been reached. Once the path-loss exponents are accurately estimated, the range estimates are obtained by using the expression (2).

Therefore, accurate range estimates can be obtained only from RSS measurements by using the RSS-based ranging technique introduced in this section and explained in detail in [5].

2.2. RTT-Based Ranging. The information related to the distance that separates two wireless nodes can be obtained by using the information of the signal propagation delay without a common time reference, but by means of the signal RTT values. In a previous work [14], a PCB was designed to measure the RTT between an MS and an anchor using the RTS/CTS two-frame exchange IEEE 802.11 mechanism. Although RTT-based ranging eliminates the error due to imperfect time synchronization because it does not need for time synchronization between wireless nodes, relative clock

drift and electronic errors still affect ranging accuracy [12]. Furthermore, the bandwidth of the transmitted signal affects ranging resolution [25]. To overcome these limitations, several RTT measurements have to be performed at each distance and a representative value of the RTT, called the RTT location estimator, has to be selected. That selection is based on the coefficient of a determination value that measures how much of the original uncertainty in the RTT measurements is explained by a model. In [26], a simple linear regression function is assumed to be the model that relates the actual distance between the two nodes involved in RTT measurements with the location estimators at each distance in LOS. Analytically,

$$\hat{d}_{\mathrm{RTT}_i} = \beta_0 + \widehat{\mathrm{RTT}}_i \beta_1, \tag{6}$$

where $\hat{d}_{\mathrm{RTT}_i}$ is the estimated distance from the MS to the anchor A_i and $\widehat{\mathrm{RTT}}_i$ is the location estimator of the actual RTT between both wireless nodes. In [26], the Hölder mean with the shape parameter of the Weibull distribution as Hölder parameter was found to be one of the best location estimators of the actual RTT when the MS and the anchor remain in LOS. The parameters β_0 and β_1 are the intercept and slope of the linear regression model, respectively. These parameters are computed so that the estimated distance best fits the actual one. They do not depend on the environment where the wireless localization system is going to be deployed, but on the wireless nodes to be used, that is, the MS and the anchors. They are previously obtained in a LOS scenario, not necessarily in the same environment where the wireless localization system is going to be deployed.

Under LOS conditions, the error in distance estimation is characterized as follows:

$$\hat{d}_{\mathrm{RTT}_i} = d_i + \epsilon_{\mathrm{RTT}}^{\mathrm{LOS}}, \tag{7}$$

where d_i is the actual distance and $\epsilon_{\mathrm{RTT}}^{\mathrm{LOS}}$ is the error in LOS. This error is defined as the difference between the estimated and the actual distances when the MS and the anchor are in LOS. This error follows a zero mean Gaussian distribution and it is a product of electronic errors (electronic noise), since a PCB is used to quantify the RTT, and also of the RTT location estimator, since it is asymptotically Gaussian and a large amount of measurements have been carried out.

Finally, the assumption that LOS propagation conditions are present in an indoor environment is an oversimplification of reality. In an indoor environment the transmitted signal could only reach the receiver through reflected, diffracted, or scattered paths. Therefore, in this kind of environments, the NLOS effect has to be considered. Thus, in an indoor environment, the distance estimate will be as follows:

$$\hat{d}_{\mathrm{RTT}_i} = d_i + \epsilon_{\mathrm{RTT}}^{\mathrm{LOS}} + \epsilon_{\mathrm{RTT}}^{\mathrm{NLOS}}, \tag{8}$$

where $\epsilon_{\mathrm{RTT}}^{\mathrm{NLOS}}$ is a random variable that represents the effect of the NLOS. The random variable $\epsilon_{\mathrm{RTT}}^{\mathrm{NLOS}}$ depends on the environment where the MS is going to be located and it has been modeled with a wide range of statistical distributions, such as Gaussian, Exponential, and Gamma, [2, 27–30], or by means of distributions obtained from specific scattering models [31]. There are several techniques that deal with the NLOS effect. The easiest method is simply to place anchors at additional locations and select those from LOS. However, one objective of this paper is to deploy a wireless localization scheme in a common and unmodified wireless network. Therefore, complex techniques that minimize the contribution of NLOS paths [32] or techniques that focus on the identification of NLOS anchors and discard them for localization [33] have to be used. Nevertheless, their reliability remains questionable in an indoor environment with abundant scatters where almost all anchors will be in NLOS. Therefore, it is crucial to use techniques that manage to introduce, in the location process, the information that actually resides in the NLOS measurements. In a previous work [26], the effect of severe NLOS was corrected from the range estimates applying the prior NLOS measurement correction (PNMC) technique [34] with dynamic estimation of the NLOS parameters [35]. The PNMC technique estimates the ratio of NLOS present in a record of time-based measurements from each anchor and corrects those measurements in a previous stage to the location process. This processing relies on the dynamic statistical estimate of the NLOS measurements present in the record. For a detailed information on the PNMC technique see [34].

Therefore, accurate range estimates can be obtained by using the RTT-based ranging technique introduced in this section and explained in detail in [26, 35].

3. Hybrid RSS-RTT Ranging Technique

The more information you have when beginning your search, the easier it will be to locate your target. From this point of view, the RTT and RSS information gathered in the MS and related to the distance to anchors will be used together to improve the ranging accuracy. The way in which the hybrid RSS-RTT ranging technique works is as follows.

Taking the RSS-based ranging technique introduced in the previous section and in order to obtain the actual path-loss exponents of the expression (5), the compatibility of distances does not have to be maximized in a global fashion, but for a set of path-loss exponents belonging to a feasible set of solutions Ψ. That is,

$$(\hat{n}_1, \hat{n}_2, \ldots, \hat{n}_M) = \arg \max_{(n_1, n_2, \ldots, n_M)} C(n_1, n_2, \ldots, n_M), \quad \text{s.t.}(n_1, n_2, \ldots, n_M) \in \Psi. \tag{9}$$

In [5] a feasible set of path-loss exponents was derived using four different constraints based on heuristic reasoning. Nevertheless, the advantage to be exploited in this paper is the fact that a simple device, such as the PCB proposed in [14], can gather both the RSS and RTT information from anchors and, consequently, RTT-based range estimates can also be used. Thus, a hybrid RSS-RTT ranging technique is proposed. It consists in imposing constraints to the RSS-based ranging technique from the RTT-based ranging estimates which correlate closely to the actual distance.

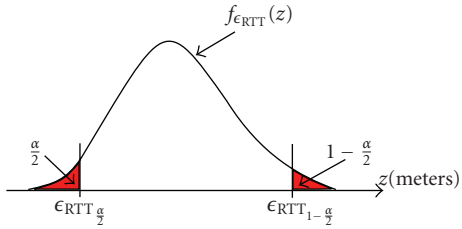

Figure 1: Graphical representation of the RTT-based constraint in a time interval (t_1, t_N).

The constraint from the RTT-based ranging estimates is as follows:

As stated in (8), $\hat{d}_{RTT_i}$, the estimated range to an anchor A_i from the RTT information, is corrupted by ϵ_{RTT}^{LOS}, a Gaussian error, and ϵ_{RTT}^{NLOS}, a NLOS error, both of them independent. As it is well known, the probability density function (PDF) of the sum of two random variables equals their PDFs' convolution. That is,

$$f_{\epsilon_{RTT}} = f_{\epsilon_{RTT}^{LOS}} * f_{\epsilon_{RTT}^{NLOS}}, \tag{10}$$

where f represents the PDF and $\epsilon_{RTT} = \epsilon_{RTT}^{LOS} + \epsilon_{RTT}^{NLOS}$. Thus, the difference between the estimated and the actual distances, $\hat{d}_{RTT_i} - d_i$, lies in the interval where the function $f_{\epsilon_{RTT}}$ is defined. However, in order to delimit that interval, with $(1-\alpha)$ probability, the estimated distance, $\hat{d}_{RTT_i}$ will be enclosed by the following expression:

$$d_i - \epsilon_{RTT_{\alpha/2}} \le \hat{d}_{RTT_i} \le d_i + \epsilon_{RTT_{1-\alpha/2}}, \tag{11}$$

and thus,

$$\hat{d}_{RTT_i} - \epsilon_{RTT_{1-\alpha/2}} \le d_i \le \hat{d}_{RTT_i} + \epsilon_{RTT_{\alpha/2}}, \tag{12}$$

where $\epsilon_{RTT_{\alpha/2}}$ and $\epsilon_{RTT_{1-\alpha/2}}$ represent the points on which the probability distribution equals probabilities $\alpha/2$ and $(1-\alpha/2)$, respectively. That is,

$$\begin{aligned} \int_{-\infty}^{\epsilon_{RTT_{\alpha/2}}} f_{\epsilon_{RTT}}(z)dz &= \frac{\alpha}{2}, \\ \int_{-\infty}^{\epsilon_{RTT_{1-\alpha/2}}} f_{\epsilon_{RTT}}(z)dz &= 1-\frac{\alpha}{2}. \end{aligned} \tag{13}$$

Figure 1 shows a possible $f_{\epsilon_{RTT}}$ in a time interval (t_1, t_N), where the actual distance d_i lies between $\hat{d}_{RTT_i} - \epsilon_{RTT_{1-\alpha/2}}$ and $\hat{d}_{RTT_i} + \epsilon_{RTT_{\alpha/2}}$ with $(1-\alpha)$ probability according to the expression (12).

By using the expression (2), range constraint (12) can be translated into path-loss constraint. That is, for $i = 1, 2, \ldots, M$

$$\begin{aligned} &\hat{d}_{RTT_i} - \epsilon_{RTT_{1-\alpha/2}} \le d_i \le \hat{d}_{RTT_i} + \epsilon_{RTT_{\alpha/2}} \\ &\iff \hat{d}_{RTT_i} - \epsilon_{RTT_{1-\alpha/2}} \le 10^{(P_{ref}-\overline{P_{R_i}})/10n_i} \le \hat{d}_{RTT_i} + \epsilon_{RTT_{\alpha/2}} \\ &\iff \frac{P_{ref} - \overline{P_{R_i}}}{10\log_{10}\left(\hat{d}_{RTT_i} - \epsilon_{RTT_{1-\alpha/2}}\right)} \\ &\qquad \ge n_i \ge \frac{P_{ref} - \overline{P_{R_i}}}{10\log_{10}\left(\hat{d}_{RTT_i} + \epsilon_{RTT_{\alpha/2}}\right)}, \end{aligned} \tag{14}$$

Furthermore, other heuristic constraint based only on RSS information can be added to the ones proposed in [5]: if $\overline{P_{R_i}}$ is the averaged RSS from the anchor A_i, let $A_1, A_2, \ldots, A_M$ be the M anchors sorted according to $\overline{P_{R_i}}$. That is,

$$\overline{P_{R_1}} \le \overline{P_{R_2}} \le \cdots \le \overline{P_{R_M}}. \tag{15}$$

Thus, certain constraints can be imposed on the distance estimates $\hat{d}_{RSS_1}, \hat{d}_{RSS_2}, \ldots, \hat{d}_{RSS_M}$. In [5] it is assumed that the estimated distance to the most powerful anchor, $\hat{d}_{RSS_1}$, is lower than the constant D_1, that is, $\hat{d}_{RSS_1} \le D_1$. As it is reasonable to assume that the most powerful anchor would be the nearest one, D_1 is chosen as the furthest distance from any possible MS position to the nearest anchor. Hence, it is reasonable to assume that the distance to the other anchors, $\hat{d}_{RSS_2}, \hat{d}_{RSS_3}, \ldots, \hat{d}_{RSS_M}$ will be enclosed by the constant D_1 and the distance that separates the anchor A_1 and the anchor A_j, $j = 2, 3, \ldots, M$, $d_{1,j}$, respectively as follows:

$$\left| d_{1,j} - D1 \right| \le \hat{d}_{RSS_j} \le d_{1,j} + D1. \quad j = 2, 3, \ldots, M. \tag{16}$$

Figure 2(a) shows a general case in which $\hat{d}_{RSS_1}$, the estimated distance to the most powerful anchor in the time interval (t_1, t_N), is lower than the parameter D_1. Figure 2(b) shows the extreme case in which $\hat{d}_{RSS_1} = D_1$ in two different scenarios, when the MS is located at the nearest point and at the furthest point from the anchor A_j with $j = 2, 3, \ldots, M$. The latter would be the case in which the equality of the expression (16) would be fulfilled.

By using the expression (2), range constraint (16) can be translated into path-loss constraint. That is, for $j = 2, 3, \ldots, M$

$$\begin{aligned} &\left| d_{1,j} - D1 \right| \le \hat{d}_{RSS_j} \le d_{1,j} + D1 \\ &\iff \left| d_{1,j} - D1 \right| \le 10^{(P_{ref}-\overline{P_{R_j}})/10n_j} \le d_{1,j} + D1 \\ &\iff \frac{P_{ref} - \overline{P_{R_j}}}{10\log_{10}\left(\left| d_{1,j} - D1 \right|\right)} \ge n_j \ge \frac{P_{ref} - \overline{P_{R_j}}}{10\log_{10}\left(d_{1,j} + D1\right)}. \end{aligned} \tag{17}$$

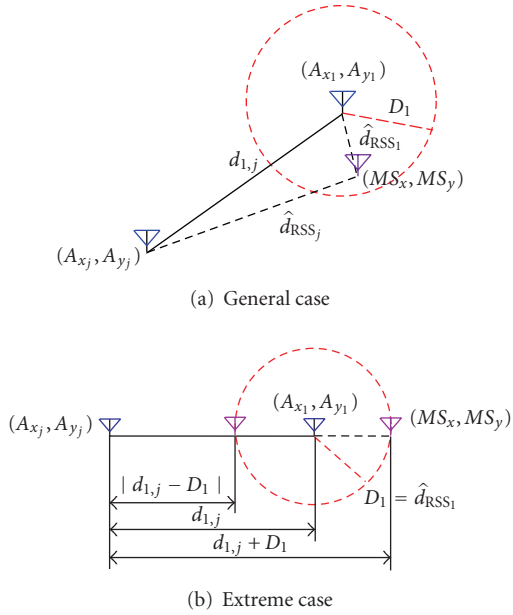

FIGURE 2: Graphical representation of the heuristic constraint D_1 in a time interval (t_1, t_N).

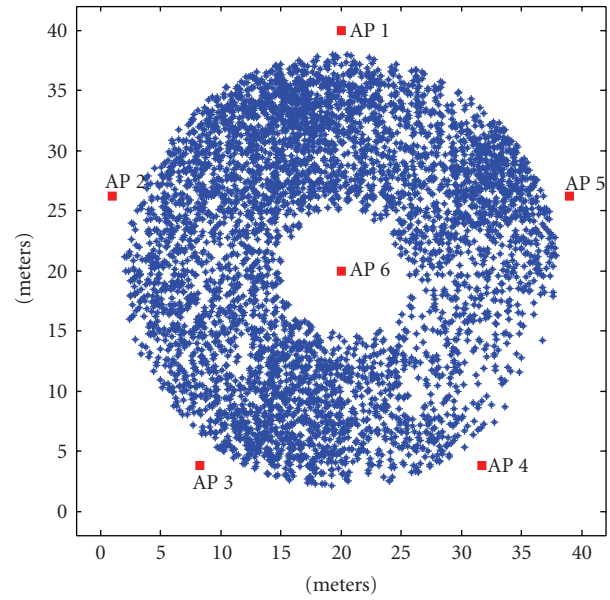

FIGURE 3: Simulation scenario ($40 \times 40\,\mathrm{m}^2$) with 6 anchors placed on the vertices and centre of a regular pentagon. The blue stars represent the actual MS positions.

Therefore, constraints (14) and (17) can be added to the feasible set of solutions Λ proposed in [5] resulting in a more restrictive set of possible path-loss exponents, Ψ.

$$\Psi = \Lambda \cup \{(\hat{n}_1, \ldots, \hat{n}_M) \ :$$

$$\frac{P_{\mathrm{ref}} - \overline{P_{R_i}}}{10 \ \log_{10}\left(\hat{d}_{\mathrm{RTT}_i} - \epsilon_{\mathrm{RTT}_{1-\alpha/2}}\right)}$$

$$\geq n_i \geq \frac{P_{\mathrm{ref}} - \overline{P_{R_i}}}{10\log_{10}\left(\hat{d}_{\mathrm{RTT}_i} + \epsilon_{\mathrm{RTT}_{\alpha/2}}\right)}, \quad i = 1, 2, \ldots, M,$$

$$\frac{P_{\mathrm{ref}} - \overline{P_{R_j}}}{10\log_{10}\left(\left|d_{1,j} - D1\right|\right)}$$

$$\geq n_j \geq \frac{P_{\mathrm{ref}} - \overline{P_{R_j}}}{10\log_{10}\left(d_{1,j} + D1\right)}, \quad j = 2, 3, \ldots, M, \tag{18}$$

where Ψ is a polyhedral set of constraints, and the expression (9) can be solved applying variants of the Levenberg-Marquardt algorithm [36]. In this paper, the centre of the polyhedron has been chosen as the initial guess for the path-loss exponents in the RSS-based range method introduced in the previous section.

3.1. Simulations. In this subsection, the accuracy improvement of the set of constraints Ψ is compared to the previous set Λ proposed in [5] by means of simulations. In order to do that, the simulation scenario consists of 5000 points corresponding with a person who is randomly walking at a constant speed between two circles with a (20,20) centre and a 5 and 18 m radius, respectively. As it can be seen in Figure 3, in the simulation scenario, 6 anchors were placed on the vertices and centre of a regular pentagon with a 20 m radius.

On one hand, according to the expression (1), for each actual position and time interval (t_1, t_N) with $N = 100$, 100, RSS values from each anchor were modeled. In the latter expression, P_{ref} was set to -56.5 dBm, and n_i was simulated as uniform random variables. In particular, $n_1 \in U(1.3, 1.7), n_2, n_3 \in U(1.7, 2.25), n_4, n_5 \in U(2.25, 3.25)$, and $n_6 \in U(3.25, 4.25)$, where $(n_1, n_2, \ldots, n_6)$ are the 6 different path-loss exponents that characterize the propagation channel from the 6 anchors sorted according to their proximity to the MS. Finally, the standard deviation of the shadow fading X was simulated as a uniform random value between 2.85 dBm and 3.45 dBm. On the other hand, according to the expression (8) for each actual position and time interval (t_1, t_N), 100 $\hat{d}_{\mathrm{RTT}}$ values from each anchor were modeled, where $\epsilon_{\mathrm{RTT}}^{\mathrm{LOS}}$ was simulated as a Gaussian random variable with zero mean and $\sigma_{\mathrm{RTT}}^{\mathrm{LOS}} = 2.3$ m, and $\epsilon_{\mathrm{RTT}}^{\mathrm{NLOS}}$ was simulated as an Exponential random variable with the parameter λ uniformly distributed, $\lambda \in U(0, 3)$. All of these simulation values were chosen as the most feasible ones based on the values obtained in previous trials with measurement equipments.

At each actual position the RSS and RTT values from the four most powerful anchors were used as inputs of the hybrid RSS-RTT ranging technique previously described. Although important information might be cut from the remaining anchors, there is one main motivation behind our taking only four anchors: the higher the number of anchors you take into account in the hybrid algorithm, the longer the time the algorithm needs to converge and find the optimal path-loss exponents. Therefore, there is a trade-off

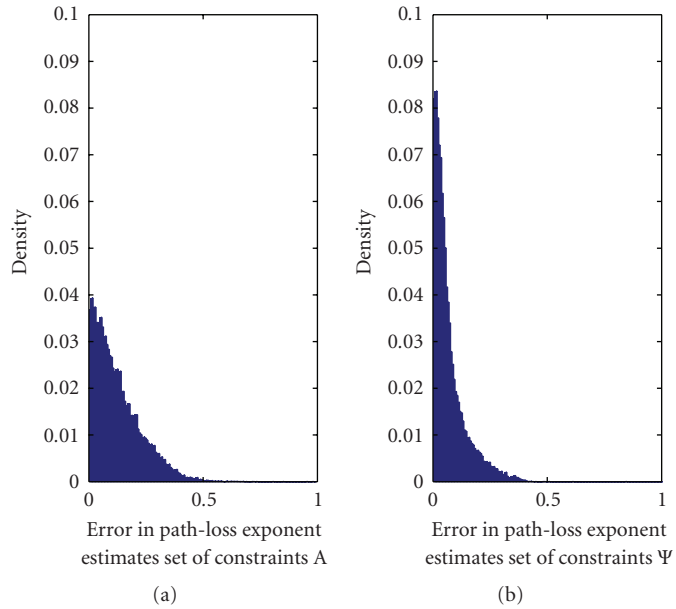

Figure 4: Histogram of errors in the path-loss exponent estimation for the different sets of constraints Λ and Ψ.

between information or accuracy in the path-loss exponent estimation and the time response.

These RSS and RTT values were used to estimate the path-loss exponents, and hence the actual distance, to each of the four anchors. The parameters needed for the set of constraints Λ were the same as the ones used in [5]. Additionally, as D_1 is the parameter that delimits the distance to the most powerful anchor, and it is reasonable to assume that the most powerful anchor will be the nearest one, the value of D_1 was chosen as the furthest distance from any possible MS position to the nearest anchor. In the simulation scenario shown in Figure 3 $D_1 = 10$ m. On the other hand, the values $\epsilon_{\mathrm{RTT}_{\alpha/2}}$ and $\epsilon_{\mathrm{RTT}_{1-\alpha/2}}$ are dynamically computed from $f_{\epsilon_{\mathrm{RTT}}}$, having taken $\alpha = 0.1$. Figure 4 shows the histogram of the 20 000 errors in the path-loss exponent estimations (5000 estimates per anchor). This error is defined as the difference between the estimated path-loss exponents and the actual ones. As it can be seen, the new set of constraints Ψ estimates the path-loss exponents more accurately than the set of constraints Λ, achieving a mean error of 0.0695 and standard deviation of 0.0722.

Furthermore, Figure 5 shows the cumulative distribution function (CDF) of the error in ranging estimates. This error is defined as the difference between the estimated range and the actual ones. In that figure, three methods are compared: the RTT-based ranging that only takes the RTT information as input data; the RSS-based ranging, set of constraints Λ, that only takes the RSS information as input data; and the hybrid RSS-RTT ranging, set of constraints Ψ, that takes the RTT and RSS information as input data. Figure 5 shows that the newly proposed hybrid method outperforms the previous ones, achieving an error lower than one meter for 50% of cases. It is important to point out that the improvement achieved by the hybrid RSS-RTT ranging method, set Ψ, is not shared in equal portions between

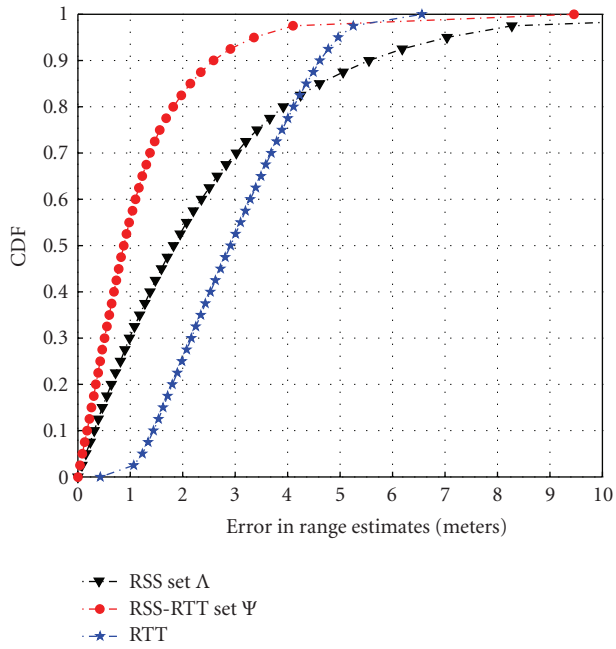

Figure 5: CDFs of errors in ranging estimate depending on the ranging method and set of constraints used.

constraints (14) and (17), but the improvement achieved by constraint (17) is marginal compared to constraint (14). Therefore, the RTT-based range constraint (14) is the main contribution to the hybrid RSS-RTT ranging method.

Finally, it is worth mentioning that none of the ranging methods described in this paper need any calibration of the environment since they are dynamic methods that try to adapt themselves to the dynamic nature of radiofrequency signals in cluttered environments, such as the indoor one.

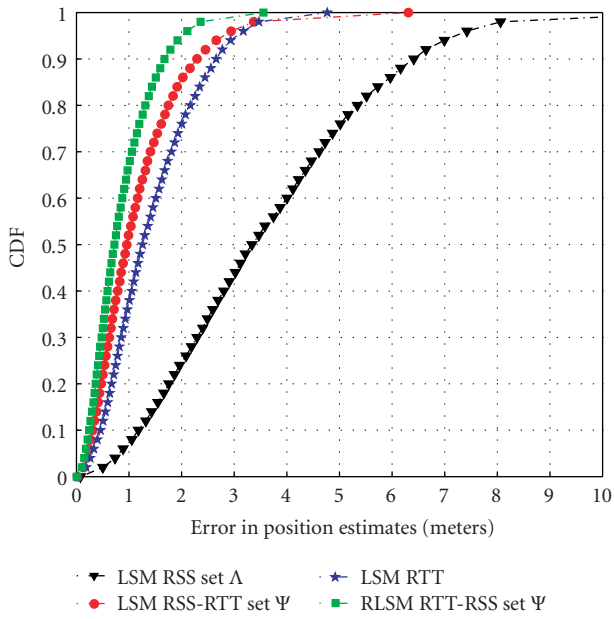

Figure 6: CDFs of errors in position estimation depending on the multilateration method and set of constraints used in the simulation scenario.

4. Hybrid RSS-RTT Multilateration Technique

After having estimated the distances between the MS and the anchors, the location of the MS can be found by multilateration, a common and well-known operation to find the MS location by using its range estimates to three or more anchors whose positions are previously known. Fortunately, additional capabilities can be included to multilateration methods to find the MS position more accurately. Since measurements outliers naturally occur in an indoor environment due to the complex propagation of the transmitted signal between the MS and the anchors, this section proposes a new multilateration technique based on a robust least-squared method with the aim of accurately finding the MS position from both the RTT and RSS-range estimates.

In two dimensions, multilateration is defined as the method to determine the intersections of M circles ($M \geq 3$). Each circle has a centre defined by the anchors position (A_{x_i}, A_{y_i}), and a radius defined by the range estimates from the MS to each anchor $(\hat{d}_i)$, both $i = 1, 2, \ldots, M$. Assuming that the number of range estimates is greater than the minimum required ($M > 3$), an over-determined system of quadratic equations has to be solved to find the MS position. However, as $\hat{d}_i$ is impacted by errors, it does not usually match the actual distance. Thus, the M circles will not cut at a single point, so the solution of that over-determined system should be found in the least-squared sense. Hence, the MS position $\mathbf{x} = [x, y]^T$ can be estimated by finding $\hat{\mathbf{x}}$ that satisfies

$$\hat{\mathbf{x}} = \arg\min_{x,y} \sum_{i=1}^{M} \left[\sqrt{(A_{x_i} - x)^2 + (A_{y_i} - y)^2} - \hat{d}_i \right]^2. \quad (19)$$

Solving problem (19) requires significant complexity and it is difficult to analyze. Therefore, instead of using the circles as the equations to determine the MS location, the radical axes of all the pairs of circles will be used [37]. The radical axis of two circles is the locus of points at which tangents drawn to both circles have the same length. It can be easily obtained by subtracting the two circles' equations involved. In this way, the complex problem of solving an over-determined system of M quadratic equations is reduced to solve an over-determined system of $(M(M-1))/2$ linear equations.

Let

$$B\mathbf{x} = \mathbf{b} \quad (20)$$

be the linear equations system defined by the radical axes with

$$B = \begin{pmatrix} (A_{x_1} - A_{x_2}) & \left(A_{y_1} - \mathrm{A}_{y_2}\right) \\ \vdots & \vdots \\ (A_{x_{M-1}} - A_{x_M}) & \left(A_{y_{M-1}} - A_{y_M}\right) \end{pmatrix}, \quad (21)$$

$$\mathbf{b} = \frac{1}{2} \begin{pmatrix} \hat{d}_2^2 - \hat{d}_1^2 - \left(A_{x_2}^2 - A_{x_1}^2\right) - \left(A_{y_2}^2 - A_{y_1}^2\right) \\ \vdots \\ \hat{d}_M^2 - \hat{d}_{M-1}^2 - \left(A_{x_M}^2 - A_{x_{M-1}}^2\right) - \left(A_{y_M}^2 - A_{y_{M-1}}^2\right) \end{pmatrix}, \quad (22)$$

where B is a matrix of $(M(M-1))/2$ rows and 2 columns described only by the anchors coordinates, while $\mathbf{b}$ is a vector of $(M(M-1))/2$ rows represented by the range estimates together with the anchor coordinates. In the least-squared sense, the solution for (20) is done via

$$\hat{\mathbf{x}} = (B^T B)^{-1} B^T \mathbf{b}, \quad (23)$$

where $\hat{\mathbf{x}}$ is an estimate of the actual MS position. Note that as $\mathbf{b}$ depends on $\hat{d}_i$ and, in general, $\hat{d}_i$ does not match the actual distance, the solution of (23) has to be found in the least-squared sense. In this paper, this method is denoted as the least-squared multilateration method (LSM).

The main drawback of using the LSM method is that all the distance estimates are weighted equally. Therefore, as it is assumed, if the number of distance estimates is greater than the minimum required to determine a two-dimensional MS location ($M > 3$), then, a new and more robust multilateration method can be defined. If $M > 3$, C groups of range estimates can be performed if and only if the number of range estimates involved in each group is not smaller than 3. That is,

$$C = \sum_{i=3}^{M} \binom{M}{i}. \quad (24)$$

Applying the LSM method to each of these combinations, C MS position estimates can be obtained and denoted as intermediate position estimates, $\hat{\mathbf{x}}_j$, $j = 1, 2, \ldots, C$. The final MS position estimate, $\hat{\mathbf{x}}$, could be obtained as the

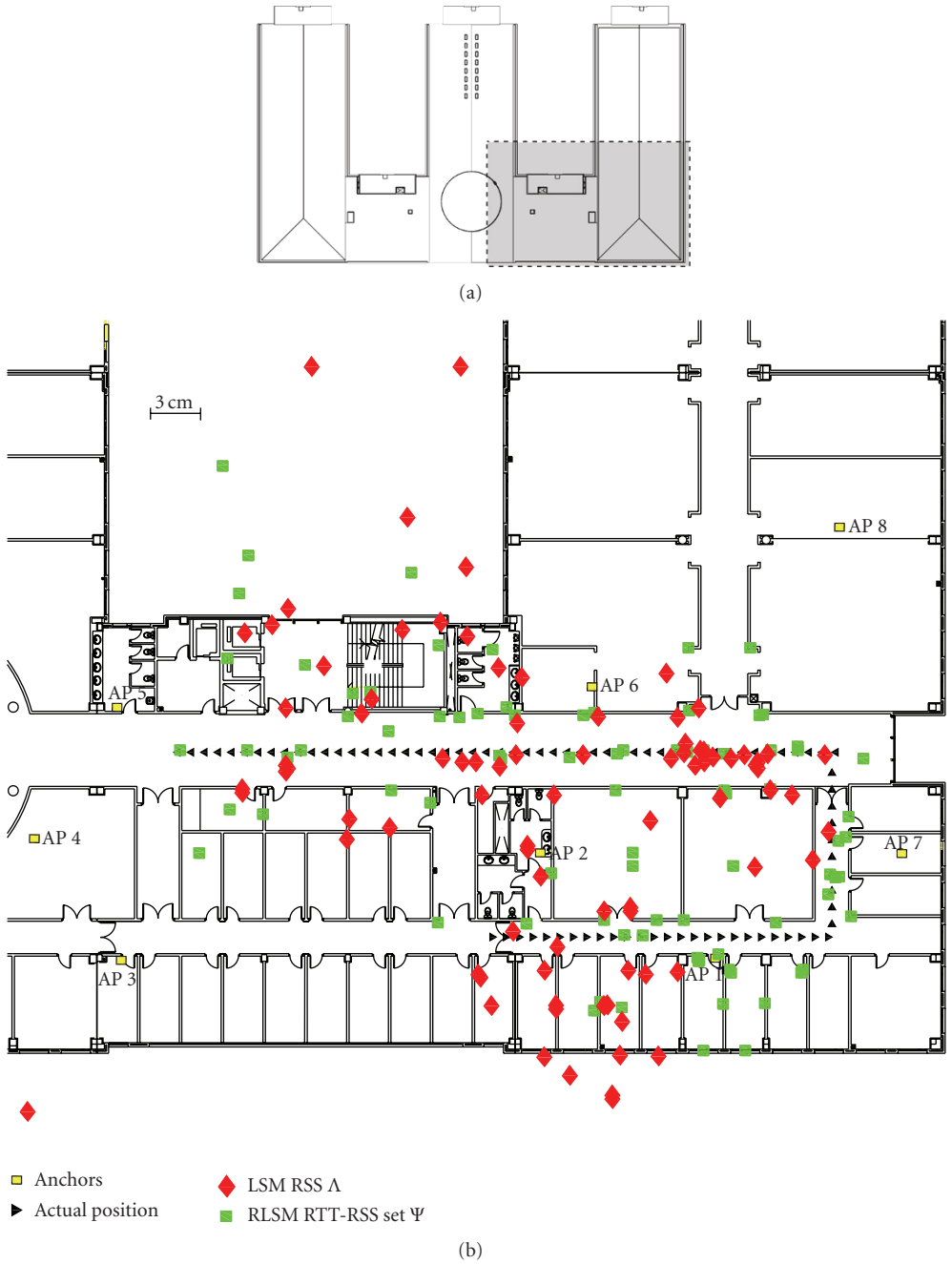

Figure 7: Position estimates on the second floor of the ETSIT.

point that minimizes the distance to all the intermediate position estimates in a robust sense. In order to do that, firstly, a vector of distances between each pair of intermediate position estimates is computed. That is

$$\mathbf{v} = [v_1, v_2, \ldots, v_i, \ldots, v_N], \quad \text{where } N = \binom{C}{2},$$

$$v_i = \left\| \hat{\mathbf{x}}_j - \hat{\mathbf{x}}_k \right\|, \quad \forall j \neq k, j, k = 1, 2, \ldots, C, \ i = 1, 2, \ldots, N. \tag{25}$$

Secondly, the median of the vector $\mathbf{v}$ is computed as a robust value in the presence of outliers. After that, the intermediate position estimates $\hat{\mathbf{x}}_j$ that are separated from more than a half of the other intermediate positions $\hat{\mathbf{x}}_k$ $(j \neq k)$ more than two times the median are removed. Therefore, the final MS position will be the point that minimizes the distance to the remaining intermediate positions. That is,

$$\hat{\mathbf{x}} = \arg \min_{x,y} \sum_{j=1}^{P} \sqrt{(\hat{x}_j - x)^2 + (\hat{y}_j - y)^2}, \tag{26}$$

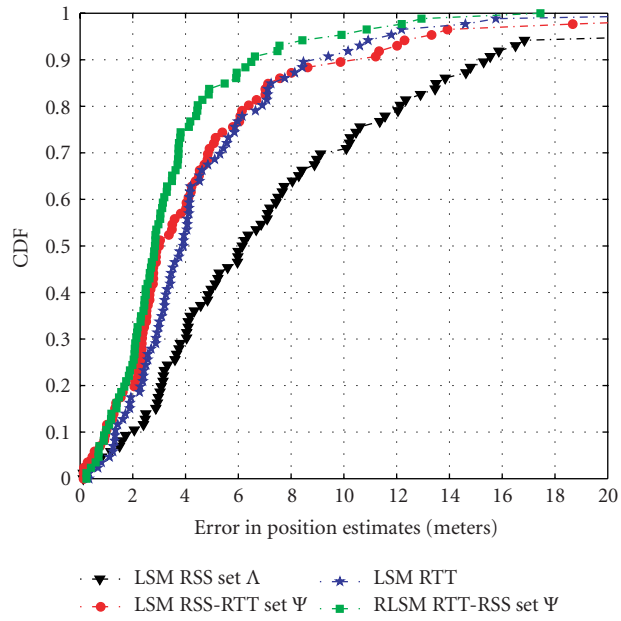

Figure 8: CDFs of errors in position estimate depending on the multilateration method and set of constraints used in a real environment, the second floor of the ETSIT building.

where P is the number of intermediate position estimates that satisfies

$$\|\hat{\mathbf{x}}_j - \hat{\mathbf{x}}_k\| < 2 \cdot \text{MED}(\mathbf{v}), \quad \forall j \neq k \text{ more than} \frac{C}{2} \text{times}, \tag{27}$$

where MED($\mathbf{v}$) denotes the median of the vector $\mathbf{v}$. This method will be denoted as the robust least-squared multilateration method (RLSM).

4.1. Simulations. In this subsection, the accuracy improvement of the hybrid localization scheme that mixes the RSS and RTT range estimates is compared to the methods that are only based on RSS or RTT range estimates by using the RLSM and LSM methods, respectively. In order to do that, the range estimates performed in the simulation scenario described in Section 3 were used. At each actual position, only the range estimates from the four most powerful anchors were used. Therefore, in order to estimate the MS position, the LSM method uses four range estimates, that is, four RSS-based or four RTT-based, while the RLSM method uses 8 range estimates, that is, four RSS-based and four RTT-based.

Figure 6 shows the CDFs of the error in the MS position estimation. This error is defined as the distance between the estimated and the actual positions. As it can be seen, the LSM method using the RSS-based, set of constraints Ψ, outperforms the same method using the set of constraints Λ, and the RTT-based method. The latter is an expected result since the RSS-based ranging method with the set of constraints Ψ outperforms the other ranging techniques. However, even better results can be achieved when mixing the RSS and RTT range estimates in the RLSM method. Figure 6 shows that a mean error lower than a meter is achieved in the MS position estimation if the RLSM method is used. Obviously, the behavior of the RLSM method is the same as the LSM method when outliers are not present as intermediate positions. Therefore, the improvement achieved by RLSM is due to mixing RSS and RTT range estimates, once the outliers were removed. It is important to point out that no tracking techniques were used.

4.2. Experimental Setup. The complete hybrid localization scheme is evaluated from the RSS and RTT measurements that were performed on the second floor of the Higher Technical School of Telecommunications (ETSIT), taking the PCB described in [14] as the measuring system. As shown in Figure 7, the campaign of measurements was carried out following a route among offices, laboratories and with a few people walking around. As anchors, 8 identical wireless access points (AP) were used with two omnidirectional rubber duck antennas vertically polarized to each other in diversity mode. The APs were configured to send a beacon frame each 100 ms at constant power on frequency channel 1 (2.412 Ghz). As MS, an IEEE 802.11 b WLAN cardbus adapter was used with two on-board patch antennas in diversity mode. Diversity circuitry determines which antenna has better reception and switches it on in a fraction of a second while it turns off the other antenna. Therefore, both antennas are never on at the same time. The PCB was connected to the WLAN cardbus adapter. Both APs and cardbus adapter can be found on most IEEE 802.11 WLANs. Figure 7 shows the multilateration points that were obtained by using the RLSM method with the previous RSS and RTT range estimates, and the LSM method with the previous RSS range estimates for the set of constraints Λ.

With the purpose of illustrating the accuracy improvement of the complete hybrid RSS-RTT localization scheme proposed in that real environment, the RLSM method is compared to the other methods cited: LSM with the RSS range estimates for the set of constraints Λ and Ψ and LSM with the RTT range estimates. Figure 8 shows the CDFs of the MS position estimation error. As it can be seen, the RLSM method outperforms the previous ones achieving a mean error lower than 3 m.

Obviously, the position accuracy could be improved using some tracking techniques, such as Kalman or particle filters, but the aim of this paper is to show the feasibility and reliability of the path-loss exponent estimates, range estimates, and MS position estimates without using any of those filtering techniques.

5. Conclusions

This paper proposes a complete hybrid localization scheme based on the RSS and RTT information, analyzing it and putting it into action in a cluttered indoor environment. A previous PCB has been taken as RSS and RTT measuring system, and an already deployed IEEE 802.11 wireless infrastructure has been used as indoor wireless technology. As a first step, a previous RSS-based ranging technique

has been improved with the RTT-based range estimates as constraints, which correlate more closely with distance. In this way, the accuracy achieved by the RSS-only and RTT-only schemes has been improved. As a second step, the MS position has been estimated using a new multilateration technique that combines the previous RSS and RTT range estimates based on a robust least-squared method. The hybrid localization scheme coupled with simulations and measurements in a cluttered indoor environment demonstrates that it outperforms the conventional RSS-based and RTT-based indoor localization schemes without using either a tracking technique or a previous calibration stage of the environment.

Hybrid localization systems have experienced a flurry of research in recent years. However, there still remain multiple areas of open research that will help systems to meet the requirements of applications that have to operate in harsh propagation environments where GNSS typically fails, such as inside buildings. These are (i) Interference mitigation: To date, the majority of research effort ignores the effects of interference on time estimation accuracy, and few papers propose robust interference mitigation techniques. (ii) Inertial Measurements Units (IMU): the integration of RSS and RTT information with IMU information, such as the one reported by accelerometers, gyroscopes, and magnetometers, could provide location estimations more precise. (iii) Secure ranging: in certain scenarios, the localization process may be subject to hostile attacks. While some works have presented secure localization algorithms (see, e.g., [38, 39]), less attention has been paid to secure ranging.

Acknowledgment

This research is partially supported by the general Board of Telecomunication of the council of public works from Castilla-León (Spain).

References

[1] K. Pahlavan and P. Krishnamurthy, *Principles of Wireless Networks: A Unified Approach*, Prentice Hall, Upper Saddle River, NJ, USA, 2002.

[2] F. Gustafsson and F. Gunnarsson, "Mobile positioning using wireless networks," *IEEE Signal Processing Magazine*, vol. 22, no. 4, pp. 41–53, 2005.

[3] C. K. Seow and S. Y. Tan, "Localization of omni-directional mobile device in multipath environments," *Progress in Electromagnetics Research*, vol. 85, pp. 323–348, 2008.

[4] N. Patwari, A. O. Hero, M. Perkins, N. S. Correal, and R. J. O'Dea, "Relative location estimation in wireless sensor networks," *IEEE Transactions on Signal Processing*, vol. 51, no. 8, pp. 2137–2148, 2003.

[5] S. Mazuelas, A. Bahillo, R. M. Lorenzo, et al., "Robust indoor positioning provided by real-time RSSI values in unmodified WLAN networks," *IEEE Journal of Selected Topics in Signal Processing*, vol. 3, no. 5, pp. 821–831, 2009.

[6] S. A. Golden and S. S. Bateman, "Sensor measurements for Wi-Fi location with emphasis on time-of-arrival ranging," *IEEE Transactions on Mobile Computing*, vol. 6, no. 10, pp. 1185–1198, 2007.

[7] L. C. Mak and T. Furukawa, "A time-of-arrival-based positioning technique with non-line-of-sight mitigation using low-frequency sound," *Journal of Electromagnetic Waves and Applications*, vol. 22, no. 5, pp. 507–526, 2008.

[8] A. Catovic and Z. Sahinoglu, "The Cramér-Rao bounds of hybrid TOA/RSS and TDOA/RSS location estimation schemes," *IEEE Communications Letters*, vol. 8, no. 10, pp. 626–628, 2004.

[9] A. Hatami and K. Pahlavan, "Hybrid TOA-RSS based localization using neural networks," in *Proceedings of the IEEE Global Telecommunications Conference (GLOBECOM '06)*, December 2006.

[10] M. Zhaounia, M. A. Landolsi, and R. Bouallegue, "Hybrid TOA/AOA approximate maximum likelihood mobile localization," *EURASIP Journal of Electrical and Computer Engineering*, vol. 2010, Article ID 942657, 5 pages, 2010.

[11] S. Venkatraman and J. Caffery Jr., "Hybrid TOA/AOA techniques for mobile location in non-line-of-sight environments," in *Proceedings of the IEEE Wireless Communications and Networking Conference (WCNC '04)*, vol. 1, pp. 274–278, March 2004.

[12] D. Dardari, A. Conti, U. Ferner, A. Giorgetti, and M. Z. Win, "Ranging with ultrawide bandwidth signals in multipath environments," *Proceedings of the IEEE*, vol. 97, no. 2, pp. 404–425, 2009.

[13] C. Fritsche and A. Klein, "Cramér-Rao lower bounds for hybrid localization of mobile terminals," in *Proceedings of the 5th Workshop on Positioning, Navigation and Communication (WPNC '08)*, vol. 1, pp. 157–164, March 2008.

[14] A. Bahillo, J. Prieto, S. Mazuelas, R. M. Lorenzo, J. Blas, and P. Fernández, "IEEE 802.11 distance estimation based on RTS/CTS two-frame exchange mechanism," in *Proceedings of the IEEE Vehicular Technology Conference*, April 2009.

[15] J. Hightower and G. Borriello, "Location systems for ubiquitous computing," *IEEE Computer*, vol. 34, no. 8, pp. 57–66, 2001.

[16] K. Pahlavan and A. H. Levesque, *Wireless Information Networks*, John Wiley & Sons, New York, NY, USA, 1995.

[17] P. Krishnan, A. S. Krishnakumar, W.-H. Ju, C. Mallows, and S. Ganu, "A system for LEASE: location estimation assisted by stationary emitters for indoor RF wireless networks," in *Proceedings of the Joint Conference of the IEEE Computer and Communications Societies (INFOCOM '04)*, vol. 2, pp. 1001–1011, March 2004.

[18] H. Hashemi, "The indoor radio propagation channel," *Proceedings of the IEEE*, vol. 81, no. 7, pp. 943–968, 1993.

[19] L. Heikki, J. Suvi, L. Timo, K. Risto, and L. Jaakko, "Experimental evaluation of location methods based on signal-strength measurements," *IEEE Transactions on Vehicular Technology*, vol. 56, no. 1, pp. 287–296, 2007.

[20] Y. Qi, *Wireless geolocation in a non-line-of-sight environment*, Ph.D. dissertation, Princeton University Press, Princeton, NJ, USA, November 2003.

[21] X. Li, "RSS-based location estimation with unknown pathloss model," *IEEE Transactions on Wireless Communications*, vol. 5, no. 12, pp. 3626–3633, 2006.

[22] J. Salo, L. Vuokko, H. M. El-Sallabi, and P. Vainikainen, "An additive model as a physical basis for shadow fading," *IEEE Transactions on Vehicular Technology*, vol. 56, no. 1, pp. 13–26, 2007.

[23] K. Levenberg, "A method for the solution of certain problems in least-squares," *Quarterly of Applied Mathematics*, vol. 2, pp. 164–168, 1944.

[24] D. Marquardt,, "An algorithm for least-squares estimation of nonlinear parameters," *SIAM Journal on Applied Mathematics*, vol. 11, pp. 431–441, 1963.

[25] V. C. Chen and H. Ling, *Time-Frequency Transforms for Radar Imaging and Signal Analysis*, Artech House, Norwood, Mass, USA, 2002.

[26] A. Bahillo, S. Mazuelas, R. M. Lorenzo, P. Fernández, J. Prieto, and E. J. Abril, "Indoor location based on IEEE 802.11 round-trip time measurements with two-step NLOS mitigation," *Progress in Electromagnetics Research B*, vol. 15, pp. 285–306, 2009.

[27] Y. Qi, H. Kobayashi, and H. Suda, "On time-of-arrival positioning in a multipath environment," *IEEE Transactions on Vehicular Technology*, vol. 55, no. 5, pp. 1516–1526, 2006.

[28] L. C. Mak and T. Furukawa, "time-of-arrival-based positioning technique with non-line-of-sight mitigation using low-frequency sound," *Journal of Electromagnetic Waves and Applications*, vol. 22, no. 5, pp. 507–526, 2008.

[29] H. Tang, Y. Park, and T. Qui, "NLOS mitigation for TOA location based on a modifed deterministic model," *Research Letters in Signal Processing*, vol. 8, no. 1, pp. 1–4, 2008.

[30] K. Yu and Y. J. Guo, "Improved positioning algorithms for nonline-of-sight environments," *IEEE Transactions on Vehicular Technology*, vol. 57, no. 4, pp. 2342–2353, 2008.

[31] S. Al-Jazzar, J. Caffery Jr., and H.-R. You, "A scattering model based approach to NLOS mitigation in TOA location systems," in *Proceedings of the IEEE Vehicular Technology Conference*, vol. 2, pp. 861–865, 2002.

[32] P.-C. Chen, "A non-line-of-sight error nitigation algorithm in location estimation," in *Proceedings of the IEEE Wireless Commununications and Networking Conference*, pp. 316–320, 1999.

[33] L. Cong and W. Zhuang, "Nonline-of-sight error mitigation in mobile location," *IEEE Transactions on Wireless Communications*, vol. 4, no. 2, pp. 560–573, 2005.

[34] S. Mazuelas, F. A. Lago, J. Blas, et al., "Prior NLOS measurement correction for positioning in cellular wireless networks," *IEEE Transactions on Vehicular Technology*, vol. 58, no. 5, pp. 2585–2591, 2009.

[35] J. Prieto, A. Bahillo, S. Mazuelas, R. M. Lorenzo, P. Fernández, and E. J. Abril, "Characterization and mitigation of range estimation errors for an rtt-based ieee 802.11 indoor location system," *Progress in Electromagnetics Research B*, vol. 15, pp. 217–244, 2009.

[36] C. Kanzow, N. Yamashita, and M. Fukushima, "Levenberg-Marquardt methods with strong local convergence properties for solving nonlinear equations with convex constraints," *Journal of Computational and Applied Mathematics*, vol. 172, no. 2, pp. 375–397, 2004.

[37] Y. Chen, J.-A. Francisco, W. Trappe, and R. P. Martin, "A practical approach to landmark deployment for indoor localization," in *Proceedings of the 3rd Annual IEEE Communications Society Conference on Sensor and Ad Hoc Communications and Networks (SECON '06)*, vol. 1, pp. 365–373, Reston, Va, USA, September 2006.

[38] Z. Li, W. Trappe, Y. Zhang, and B. Nath, "Robust statistical methods for securing wireless localization in sensor networks," in *Proceedings of the 4th International Symposium on Information Processing in Sensor Networks*, pp. 91–98, April 2005.

[39] Y. Zhang, W. Liu, W. Lou, and Y. Fang, "Location-based compromise-tolerant security mechanisms for wireless sensor networks," *IEEE Journal on Selected Areas in Communications*, vol. 24, no. 2, pp. 247–260, 2006.